The Dual-Antigen Ad5 COVID-19 Vaccine Delivered as an Intranasal Plus Subcutaneous Prime Elicits Th1 Dominant T-Cell and Humoral Responses in CD-1 Mice

Adrian Rice[1ϕ], Mohit Verma[1ϕ], Annie Shin[1], Lise Zakin[1], Peter Sieling[1], Shiho Tanaka[1], Joseph Balint[1], Kyle Dinkins[1], Helty Adisetiyo[1], Brett Morimoto[1], Wendy Higashide[1], Justin Taft[2,3], Rosheel Patel[2,3], Sofija Buta[2,3,4], Marta Martin-Fernandez[2,3,4,5,6], Dusan Bogunovic[2,3,4,5,6], Patricia Spilman[1], Elizabeth Gabitzsch[1], Jeffrey T. Safrit[1], Shahrooz Rabizadeh[1], Kayvan Niazi[1], Patrick Soon-Shiong[1]*

[ϕ] These authors contributed equally

[1]ImmunityBio, Inc., 9920 Jefferson Blvd, Culver City, CA 90232, USA

[2]Center for Inborn Errors of Immunity, [3]Department of Pediatrics, [4]Precision Immunology Institute, [5]Mindich Child Health and Development Institute, [6]Department of Microbiology, Icahn School of Medicine at Mount Sinai, 1 Gustave Lane, Levy Place, New York, NY 10029-5674, USA

*Corresponding author: Patrick@NantWorks.com

ABSTRACT

In response to the need for an efficacious, thermally-stable COVID-19 vaccine that can elicit both humoral and cell-mediated T-cell responses, we have developed a dual-antigen human adenovirus serotype 5 (hAd5) COVID-19 vaccine in formulations suitable for subcutaneous (SC), intranasal (IN), or oral delivery. The vaccine expresses both the SARS-CoV-2 spike (S) and nucleocapsid (N) proteins using an hAd5 platform with E1, E2b, and E3 sequences deleted (hAd5[E1-, E2b-, E3-]) that is effective even in the presence of hAd5 immunity. In the vaccine, S is modified (S-Fusion) for enhanced cell-surface display to elicit humoral responses and N is modified with an Enhanced T-cell Stimulation Domain (N-ETSD) to direct N to the endosomal/lysosomal pathway to increase MHC I and II presentation. Initial studies using subcutaneous (SC) prime and SC boost vaccination of CD-1 mice demonstrated that the hAd5 S-Fusion + N-ETSD vaccine elicits T-helper cell 1 (Th1) dominant T-cell and humoral responses to both S and N. We then compared SC to IN prime vaccination with either an SC or IN boost post-SC prime and an IN boost after IN prime. These studies reveal that IN prime/IN boost is as effective at generating Th1 dominant humoral responses to both S and N as the other combinations, but that the SC prime with either an IN or SC boost elicits greater T cell responses. In a third study to assess the power of the two routes of delivery when used together, we used a combined SC plus IN prime with or without a boost and found the combined prime alone to be as effective as the combined prime with either an SC or IN boost in generating both humoral and T-cell responses. The findings here in CD-1 mice demonstrate that combined SC and IN prime-only delivery has the potential to provide broad immunity – including mucosal immunity – against SARS-CoV-2 and supports further testing of this delivery approach in additional animal models and clinical trials.

50 **INTRODUCTION**

51 In response to the need for a COVID-19 vaccine that is safe, effective, and suitable for global
52 distribution, we have developed the dual antigen hAd5 S-Fusion + N-ETSD vaccine including
53 formulations for subcutaneous (SC), oral, and intranasal (IN) delivery. The vaccine comprises the
54 SARS-CoV-2 spike (S) protein optimized for cell surface expression (S-Fusion) [1] to increase
55 humoral responses and the nucleocapsid protein with an Enhanced T-cell Stimulation Domain (N-
56 ETSD) to target N to the endosomal/lysosomal cellular compartment to enhance MHC I and II
57 presentation.[2]

58 The vaccine antigens are delivered using a human adenovirus serotype 5 (hAd5) vector with
59 deletions in the E1, E2b, and E3 gene regions (hAd5 [E1-, E2b-, E3-]; Supplementary Fig. S1A).[3]
60 Specifically, removal of the E2b regions confers advantageous immune properties by minimizing
61 immune responses to Ad5 viral proteins such as viral fibers, [4] thereby eliciting potent immune
62 responses to specific antigens in patients with pre-existing adenovirus (Ad) immunity. [5,6] Since
63 these deletions allow the hAd5 platform to be efficacious even in the presence of existing Ad
64 immunity, this platform enables relatively long-term antigen expression without significant
65 induction of anti-vector immunity. It is therefore also possible to use the same vector/construct for
66 homologous prime-boost therapeutic regimens.[7] Importantly, this next generation Ad vector has
67 demonstrated safety in over 125 patients with solid tumors. In these Phase I/II studies, CD4+ and
68 CD8+ antigen-specific T cells were successfully generated to multiple somatic antigens (CEA,
69 MUC1, brachyury) even in the presence of pre-existing Ad immunity.[5 8]

70 SARS-CoV-2 is an enveloped positive sense, single-strand RNA β coronavirus primarily
71 composed of four structural proteins - spike (S), nucleocapsid (N), membrane (M), and envelope
72 (E) – as well as the viral membrane and genomic RNA. The S glycoprotein [9-11] is displayed as a
73 trimer on the viral surface, whereas N is located within the viral particle (Supplementary Fig. S1B).

74 Spike initiates infection by the SARS-CoV-2 virus by interaction of its receptor binding domain
75 (RBD) with the human host angiotensin-converting enzyme 2 (ACE2) expressed on the surface of
76 cells in the respiratory system, including alveolar epithelial cells, [12] as well as cells in the digestive
77 tract.

78 The majority of current SARS-CoV-2 vaccines under development deliver only the S antigen
79 because antibodies raised against S RBD are expected to neutralize infection.[13-15] Reliance on S as
80 the sole vaccine antigen is not without risk, however, particularly in the face of the rapidly
81 dominating variants including the B.1.351 variant expressing E484K, K417N, and N501Y
82 mutations; [16] the B.1.1.7 variant (N501Y); [17,18] and the Cal.20.C L452R variant [19] all of which
83 have altered RBD sequences that may not be as effectively recognized by antibodies generated in
84 response to first-wave S-based vaccines.

85 To lessen the risk of single-antigen delivery and to broaden protective immune responses, we
86 included the N protein in our hAd5 S-Fusion + N-ETSD vaccine (Supplementary Fig. S1C). N is
87 a highly conserved and antigenic SARS-CoV-2-associated protein that has been studied previously
88 as an antigen in coronavirus vaccine design for SARS-CoV.[20-23] N associates with viral RNA and
89 has a role in viral RNA replication, virus particle assembly, and release.[24,25] Studies have shown
90 that nearly all patients infected with SARS-CoV-2 have antibody responses to N.[26,27] Furthermore,
91 another study reported that most, if not all, COVID-19 survivors tested were shown to have N-
92 specific CD4+ T-cell responses.[15]

93 The ability of N to elicit vigorous T-cell responses highlights another advantage of the addition
94 of N. A robust T-cell response to vaccination is at least as important as the production of antibodies
95 [28] and should be a critical consideration for COVID-19 vaccine efficacy. First, humoral and T-cell
96 responses are highly correlated, with titers of neutralizing antibodies being proportional to T-cell
97 levels, suggesting the T response is necessary for an effective humoral response.[29] It is well

98 established that the activation of CD4+ T helper cells enhances B-cell production of antibodies.
99 Second, virus-specific CD4+ and CD8+ T cells are widely detected in COVID-19 patients,[30] based
100 on findings from patients recovered from the closely-related SARS-CoV, and there are reports that
101 such T cells persist for at least 6–17 years, suggesting that T cells may be an important part of
102 long-term immunity.[31-33] These T-cell responses were predominantly to N, as described in Le Bert
103 *et al.*, who found that in all 36 convalescent COVID-19 patients in their study, the presence of
104 CD4+ and CD8+ T cells recognizing multiple regions of the N protein could be demonstrated.[33]
105 They further examined blood from 23 individuals who had recovered from SARS-CoV and found
106 that the memory T cells acquired 17 years ago also recognized multiple proteins of SARS-CoV-2.
107 These findings emphasize the importance of designing a vaccine with the highly conserved
108 nucleocapsid present in both SARS-CoV and SARS-CoV-2. Third, recovered patients exposed to
109 SARS-CoV-2 have been found without seroconversion, but with evidence of T-cell responses.[34]
110 The T-cell based responses become even more critical given the finding in at least one study that
111 neutralizing antibody titers decline in some COVID-19 patients after about 3 months.[35] The
112 importance of both S and N was highlighted by Grifoni *et al*.[15] who identified both S and N
113 antigens as *a priori* potential B and T-cell epitopes for the SARS-CoV virus that shows close
114 similarity to SARS-CoV-2 that are predicted to induce both T and B cell responses.

115 Additional considerations for vaccine design beyond the choice of antigens, include the
116 practicality of global distribution and the ability to generate mucosal immunity that provides the
117 highest probability of preventing transmission. While the mRNA-based vaccines have shown
118 excellent efficacy, [36,37] their requirement for extremely cold storage has presented a challenge,
119 particularly for developing countries. Our hAd5 [E1-, E2b-, E3-] platform-based vaccine
120 overcomes the need for super-cold storage, with the injectable and IN formulations requiring only

121 -20°C (up to one year) or 2-8°C (up to one month) storage. The oral formulation has a further
122 advantage of being stable at room temperature.

123 IN or oral vaccine delivery also offers the potential for conferring mucosal immunity. SARS-
124 CoV-2 is a mucosal virus [38,39] that in most instances of infections, initiates infection by entry to
125 the nose and mouth. Similarly, it's most efficient route of transmission is by respiratory droplets
126 that are then transmitted to other persons.[40] Thus a vaccine that also elicits protective mucosal
127 responses mediated by IgA is more likely to reduce transmission as compared to systemic, IgG-
128 only humoral and T-cell responses. [41]

129 It was our goal in the studies presented herein to confirm enhanced cell surface expression of
130 S-Fusion as compared to S-WT (the localization of N-ETSD to endo/lysosomes is demonstrated
131 in Sieling *et al.* 2020 [2]) in *in vitro* studies, then assess humoral and T cell responses *in vivo* studies
132 in CD-1 mice. In mice, first the immune responses to SC prime and SC boost vaccination were
133 determined, then SC and IN prime delivery were compared. In a third experiment, the two routes
134 of delivery were combined in a single boost to ascertain if together optimal immune responses
135 could be achieved that may not necessarily be dependent upon a boost.

136 In all three study paradigms - SC prime with SC boost study, SC versus IN prime with boost,
137 and combined SC plus IN prime with or without boost - immunization of CD-1 mice with the hAd5
138 S Fusion + N-ETSD vaccine elicited Th1 dominant, virus-neutralizing humoral responses against
139 S. Both CD4+ and CD8+ T-cell responses to SARS-CoV-2 S and N peptide pools were also seen,
140 with cytokine production being greater overall in response to N peptides in all studies. Potent
141 neutralization of SARS-CoV-2 by sera from vaccinated mice in all studies was confirmed by a
142 surrogate neutralization assay. [42] While all dosing paradigms produced broad immune responses,
143 perhaps the most significant and compelling finding was that a single prime administration by

144 combined SC and IN dosing generated immune responses that were at least as great as dosing
145 regimens that included a boost.
146
147 **RESULTS**
148 **S-Fusion enhances cell-surface display of conformationally-relevant spike**
149 Before initiation of *in vivo* studies in mice, our goal of enhancing cell-surface display of S was
150 confirmed by transfection of HEK-293T cells with hAd5 S wild type (S WT), S-WT plus N-ETSD,
151 S-Fusion alone, and S-Fusion plus N-ETSD followed by flow cytometric analysis of anti-S
152 receptor binding domain (S RBD) antibody binding. As shown in Supplementary Figure S2A-E,
153 antibody binding was enhanced with S-Fusion as compared to S-WT and was found to be the
154 highest for hAd5 S-Fusion plus N-ETSD. This enhanced cell surface expression was further
155 confirmed by binding of recombinant ACE2, which was also the highest for hAd5 S-Fusion + N-
156 ETSD (Supplementary Fig. S2F-H). The binding of both antibodies and ACE2 to S as expressed
157 by the vaccine not only confirms increased surface expression, it verifies conformational relevance
158 of the surface-displayed S protein.
159 ***In Vivo* Studies in Mice**
160 **Mice generated both anti-S and anti-N antibodies in response to SC prime, SC boost**
161 **vaccination**
162 In this initial study to test an SC hAd5 S-Fusion + N-ETSD prime followed by an SC boost,
163 CD-1 female mice received 1 x 10^{10} viral particles (VP) of either hAd5 Null or the vaccine, both
164 n = 5, on Days 0 and 21. Mice were euthanized and tissue collected for analysis on Day 28 (Fig.
165 1A).

166 Vaccinated mice generated anti-S antibodies that were shown to be neutralizing in surrogate
167 and live virus assays (Fig. 1B, C, and D, respectively). Vaccinated mice also generated anti-N
168 antibodies (Fig. 1E), and both the anti-S and anti-N antibodies were Th1 dominant (Fig. 1F).
169 Our neutralization data with live SARS-CoV-2 virus demonstrated the potency of the antibody
170 response generated following vaccination with hAd5 S-Fusion + N-ETSD, with evidence of high
171 neutralization even at a high dilution factor. In addition, a synergistic effect of pooled sera was
172 evident, with potent neutralization even greater than control convalescent serum at ≥ 1:1,000
173 dilution.

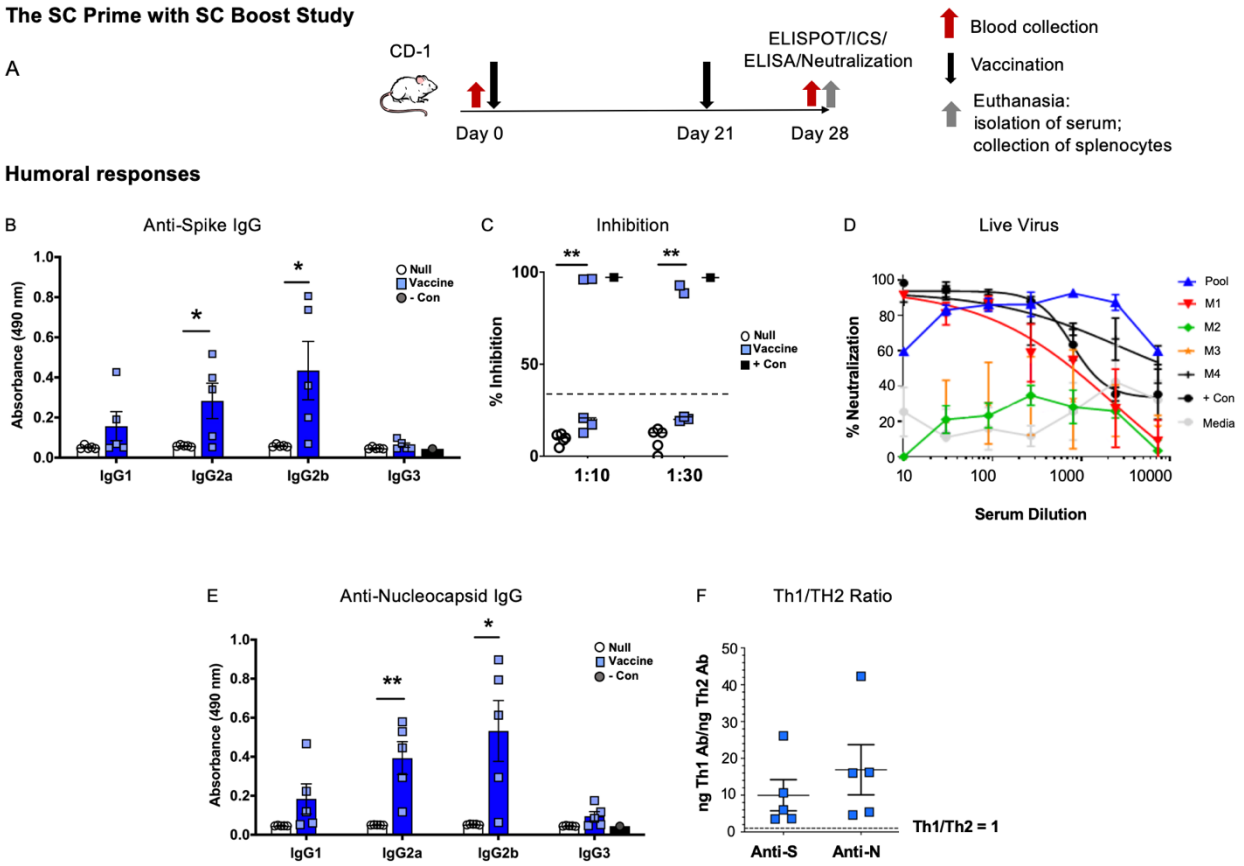

174
175 **Fig. 1** *Humoral responses in the SC prime, SC boost study*. (A) CD-1 mice received either hAd5
176 Null or the hAd5 S-Fusion + N-ETSD vaccine (both n = 5) on Day 0 and Day 21 by subcutaneous
177 (SC) injection and were euthanized for tissue collection on Day 28. (B) Anti-spike (S) antibody
178 levels in sera by isotype are shown (dilution 1:30); (C) results of the surrogate spike receptor
179 binding domain (S RBD): angiotensin-converting enzyme 2 (ACE2) binding assay where
180 inhibition of 35% or greater is associated with neutralization; and (D) percent neutralization in the
181 live virus assay are shown for the 4 vaccinated mice with assessible sera as well as pooled sera

182 from these mice. (E) Anti-nucleocapsid (N) antibody levels (dilution 1:90) by isotype and (F) the
183 T helper cell 1 (Th1)/Th2 ratios for both anti-S and anti-N antibodies with a ratio greater than 1
184 representing Th1 dominance. Statistics performed using an unpaired two-tailed Student's t-test
185 where *$p < 0.05$ and **$p \leq 0.01$.
186
187 **N peptides elicited strong CD4+ T-cell, but S peptides elicited strong CD8+ T-cell responses**
188 **in SC prime, SC boost vaccinated mice**

189 Intracellular cytokine staining (ICS) revealed that the N peptide pool stimulated interferon-γ
190 (IFN-γ) and tumor necrosis factor alpha (TNF-α) production in selected CD4+ T-lymphocytes
191 from vaccinated but not hAd5 Null mice (Fig. 2A and B). Conversely, the S1 peptide pool
192 (containing S RBD) elicited higher IFN-γ/TNF-α production in CD8+ T-lymphocytes than the N
193 peptide pool (Fig. 2C and D). ELISpot showed N peptides stimulated higher IFN-γ secretion than
194 the S1 peptide pool, but cytokine secretion was greater with both stimuli in T-cells from vaccinated
195 mice as compared to Null (Fig. 2E). IL-4 secretion was very low, therefore the T-cell responses,
196 like humoral responses, were Th1 dominant with the IFN-γ/IL-4 ratio being >1 in 4 of 5 vaccinated
197 mice (Fig. 2F and G).

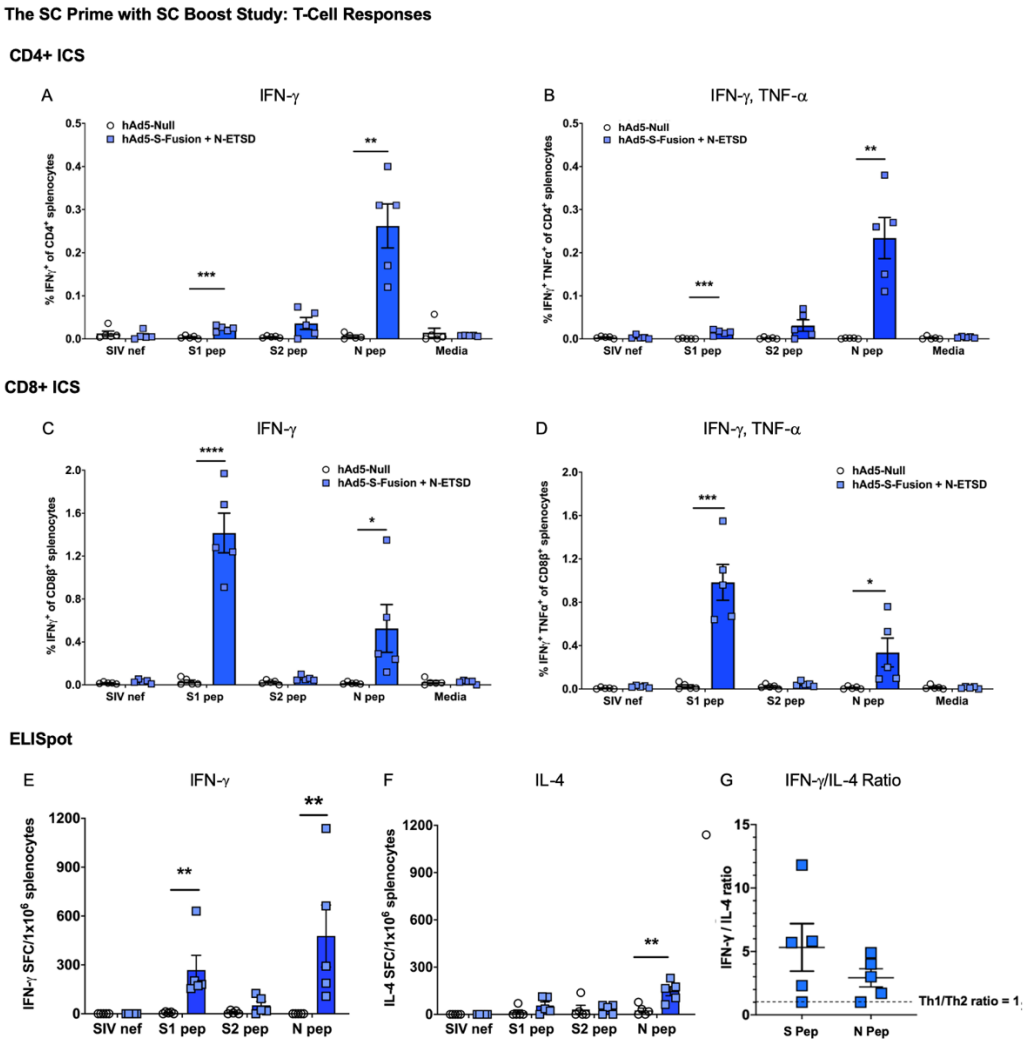

198
199 **Fig. 2** *T-cell responses in SC prime, SC boost hAd5 S-Fusion + N-ETSD vaccinated mice.*
200 Production of interferon-γ (IFN-γ) for (A) CD4+ and (C) CD8β+ T lymphocytes; and IFN-γ/tumor
201 necrosis factor α (TNF-α) by (B) CD4+ and (D) CD8β+ T lymphocytes by intracellular cytokine
202 staining (ICS) is shown. ELISpot detection of (E) IFN-γ and (F) interleukin-4 (IL-4) by T-
203 lymphocytes is shown. In both ICS and ELISpot, cytokine production is stimulated by exposure
204 to S1, S2 or N peptide pools; media only and SIV nef are negative controls. (G) The IFN-γ/IL-4
205 ratio > 1 reflects Th1 dominance. Statistical analyses performed using an unpaired, two-tailed
206 Student's t-test where *$p < 0.05$, **$p \leq 0.01$, and ***$p \leq 0.001$.
207
208 **IN prime with an IN boost vaccination with hAd5 S-Fusion + N-ETSD elicited humoral**
209 **responses that were as good or better than SC prime with either SC or IN boost**
210 To both enhance and broaden immune responses by generation of mucosal immunity, we next
211 performed a study wherein the prime delivery by either SC and intranasal (IN) routes would be
212 compared when followed by either an SC or IN boost. The design of the SC versus IN prime with

213 SC or IN boost study is shown in Figure 3A. There were 4 groups of CD-1 mice: untreated, SC
214 prime followed by SC boost (SC > SC), IN prime followed by IN boost (IN > IN), and SC prime
215 followed by IN boost (SC > IN). SC doses were administered at 1 x 10^{10} VP and IN doses were
216 administered at 1 x 10^{9} VP. The untreated group was n = 4, SC > SC and SC > IN were n = 8 and
217 IN > IN n =7. Mice received the priming doses on Day 0 and boosting doses on Day 21. All mice
218 were euthanized on Day 28 and tissue including blood for serum, spleens for T cells, and lung
219 tissue collected for analyses.

220 Mice in all vaccinated groups produced anti-S IgG and overall, levels were the highest in sera
221 from IN > IN group mice (Fig. 3B). Sera were highly neutralizing as reflected by high inhibition
222 in the surrogate virus neutralization assay (Fig. 3C). Anti-N IgG was also detected in sera from all
223 vaccinated mice, with the levels being very similar between vaccinated groups (Fig. 3D).

224 Similar to the findings for sera, anti-S IgG was detected in lung homogenate of all vaccinated
225 mice and was higher overall for the IN > IN group (Fig. 3E). Lung homogenate from all IN > IN
226 group mice showed high inhibition in the surrogate neutralization assay, whereas homogenate from
227 4 mice in the SC > SC boost group did not surpass the 35% level of inhibition that is associated
228 with viral neutralization (Fig. 3F). In lung homogenate, anti-N IgG showed a trend to higher in the
229 SC > IN group (Fig. 3G). Not unexpectedly, both anti-S and anti-N IgA levels in lung homogenate
230 were highest in the IN > IN boost group (Fig. 3H). Furthermore, the anti-S and anti-N responses
231 in both sera and lung were highly Th1 dominant for all vaccinated groups (Fig. 3I).

The SC *versus* IN Prime with IN or SC Boost Study

A

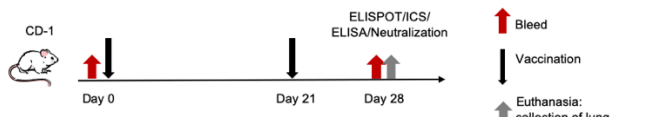

N #	Prime Route	Dose	Boost Route	Dose
4	n/a	n/a		
8	SC	1×10^{10} VP	SC	1×10^{10} VP
7	IN	1×10^{9} VP	IN	1×10^{9} VP
8	SC	1×10^{10} VP	IN	1×10^{9} VP

Humoral Responses

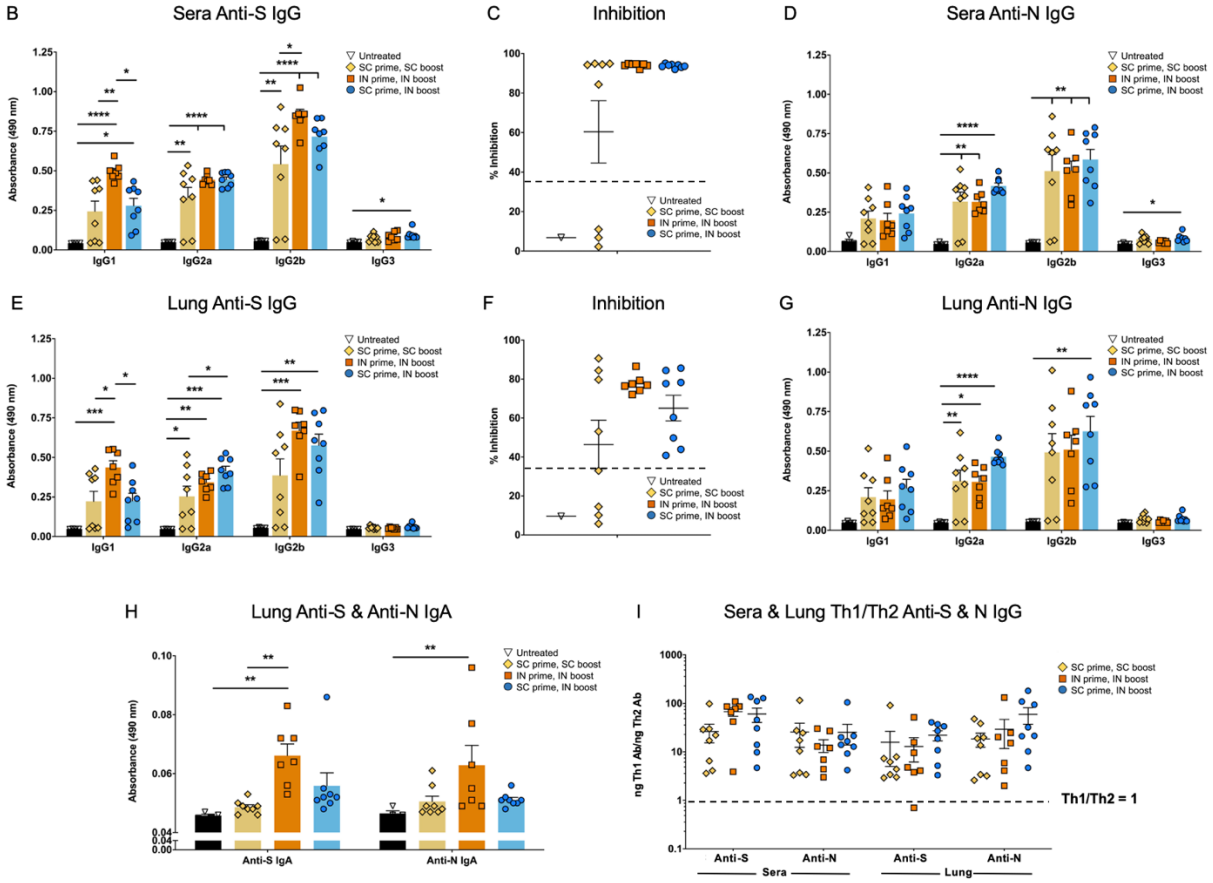

Fig. 3 *Humoral responses in the SC versus IN prime with SC or IN boost study*. (A) CD-1 mice were untreated (n = 4) or received an SC prime, SC boost (n = 8); IN prime, IN boost (n = 7); or SC prime, IN boost (n = 8). (B) Sera levels of anti-S antibodies (dilution 1:30) by subtype are shown and (C) percent inhibition in the surrogate neutralization assay of ACE2:S RBD binding wherein inhibition of 35% or greater is associated with neutralization of viral infection. (D) Levels of anti-N IgG in sera (dilution 1:270). (E) Anti-S IgG by subtype (dilution 1:30) and (F) neutralization by lung homogenate. (G) Lung anti-N IgG levels (dilution 1:30). (H) Both anti-S and anti-N IgA in lung homogenate. (I) The Th1/Th2 ratios for sera and lung anti-S and anti-N antibodies where values greater than 1 represent Th1 dominance. Statistical analyses performed using One-way ANOVA with Tukey's post-hoc analysis comparing each group to every other group where *$p < 0.05$; **$p \leq 0.01$; ***$p \leq 0.001$; and ****$p \leq 0.0001$.

245 **Both CD4+ and CD8+ T-cell responses were greater to N than S, and higher with SC delivery**

246 Intracellular cytokine staining (ICS) of IFN-γ (Fig. 4A, D); IFN-γ, TNF-α (Fig. 4B, E), and
247 IFN-γ, TNF-α, interleukin-2 (IL-2) (Fig. 4C, F) showed the highest mean values for the SC > SC
248 boost and SC > IN vaccinated groups with responses to the N peptide pool trending higher for both
249 CD4+ and CD8+ T cells. This was somewhat in contrast with the findings of the first SC > SC
250 boost study (study 1 above) where CD8+ T-cell responses were greater to the S1 peptide pool (Fig.
251 2C), however, variation is expected in outbred CD-1 mice and robust CD8+ responses to both S
252 and N were detected in SC > SC mice from each study. While the differences were not statistically
253 significant due to variation among individual mice, overall the IN > IN boost group had a reduced
254 population of CD8+ cells capable of accumulating IFN-γ (Fig. 4D) and IFN-γ + TNF-α (Fig. 4E)
255 in response to S and N peptide stimulation.

256 ELISpot findings were similar, with higher responses seen for the SC > SC and SC > IN
257 groups when compared to the IN > IN group, and the highest responses were found to be specific
258 to the N peptide pool (Fig. 4G). Interleukin-4 (IL-4) secretion in ELISpot was very low for all
259 groups (Fig. 4H), therefore the IFN-γ/IL-4 ratios were above 1 for almost all vaccinated mice in
260 response to both S and N peptide pools (Fig. 4I).

261 The T-cell responses in this study suggested an important contribution of SC delivery to T cell
262 responses.

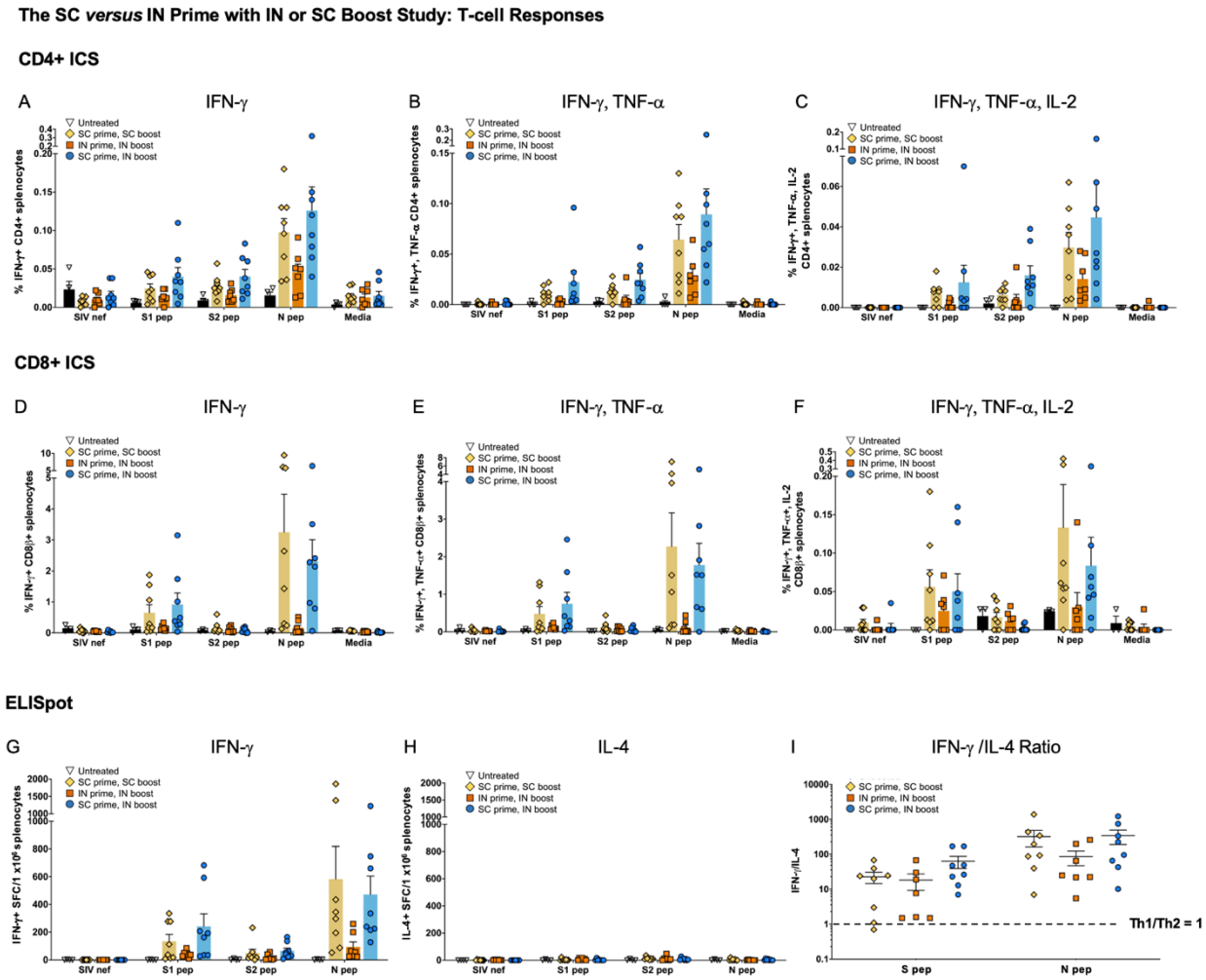

Fig. 4 *Both CD4+ and CD8+ T cells respond the nucleocapsid peptides in SC versus IN prime study with SC or IN boost*. Cytokine production in response to S1, S2 and N peptide pools as detected by Intracellular cytokine staining (ICS) of (A) Interferon-γ (IFN-γ); (B) IFN-γ and tumor necrosis factor α (TNF-α); and (C) IFN-γ, TNF-α, and interleukin-2 (IL-2) production by CD4+ is shown. ICS (D-F) IFN-γ; IFN-γ, TNF-α; and IFN-γ, TNF-α, and IL-2 for CD8+ T cells is shown. Some outliers by the Grubb's test were removed. ELISpot for (G) IFN-γ and (H) interleukin-4 (IL-4) secretion in response to the peptide pools is shown. SIV nef is a negative control. (I) The IFN-γ/IL-4 ratio showing T helper cell 1 dominance. Statistical analyses performed using One-way ANOVA with Dunnett's post-hoc comparison of each treatment group to untreated for each peptide pool was performed but did not reveal statistically significant differences due to individual variation amongst mice.

Prime-only delivery by combined SC and IN dosing elicits humoral responses that are as good or better than those with a boost

To leverage both the humoral responses effectively elicited by IN delivery with the T-cell responses that were greater with SC delivery, we then tested prime delivery by a combination of

280 the SC and IN routes, with either IN or SC boosts. This study design is shown in Figure 5A. There
281 were 5 groups of CD-1 mice: untreated, an SC prime at 1 x 10^{10} viral particles (VP) without boost
282 (SC > no boost), a combined 9 x 10^{9} VP SC plus 1 x 10^{9} VP IN prime (SC/IN) without boost
283 (SC/IN > no boost), a combined SC/IN prime with 1 x 10^{9} VP IN boost (SC/IN > IN), and a
284 combined SC/IN prime with a 1 x 10^{10} VP SC boost (SC/IN > SC). The untreated group was n =
285 4 and all vaccinated groups were n = 7. Mice received the prime on Day 0 and in appropriate
286 groups, the boost on Day 21. All mice were euthanized on Day 35 and tissue including blood for
287 serum, spleens for T cells, and lung tissue collected for analyses. Note this euthanasia day is one
288 week later than the two studies described above (Figs. 1A and 3A), which was a change meant to
289 better characterize humoral responses at a time point at which we expected cell-mediated responses
290 to remain high based on our prior work with this vaccine platform.

291 The combined SC/IN > no boost regimen was just as effective in eliciting neutralizing anti-S
292 IgG and anti-N IgG antibody production in both sera (Fig. 5B-D) and lung (Fig. 5E-G) as either
293 the SC/IN > IN or SC/IN > SC regimens. SC > no boost gave significantly lower humoral
294 responses (Fig. 5B-G). All humoral responses were Th1 dominant (Fig. 5H).

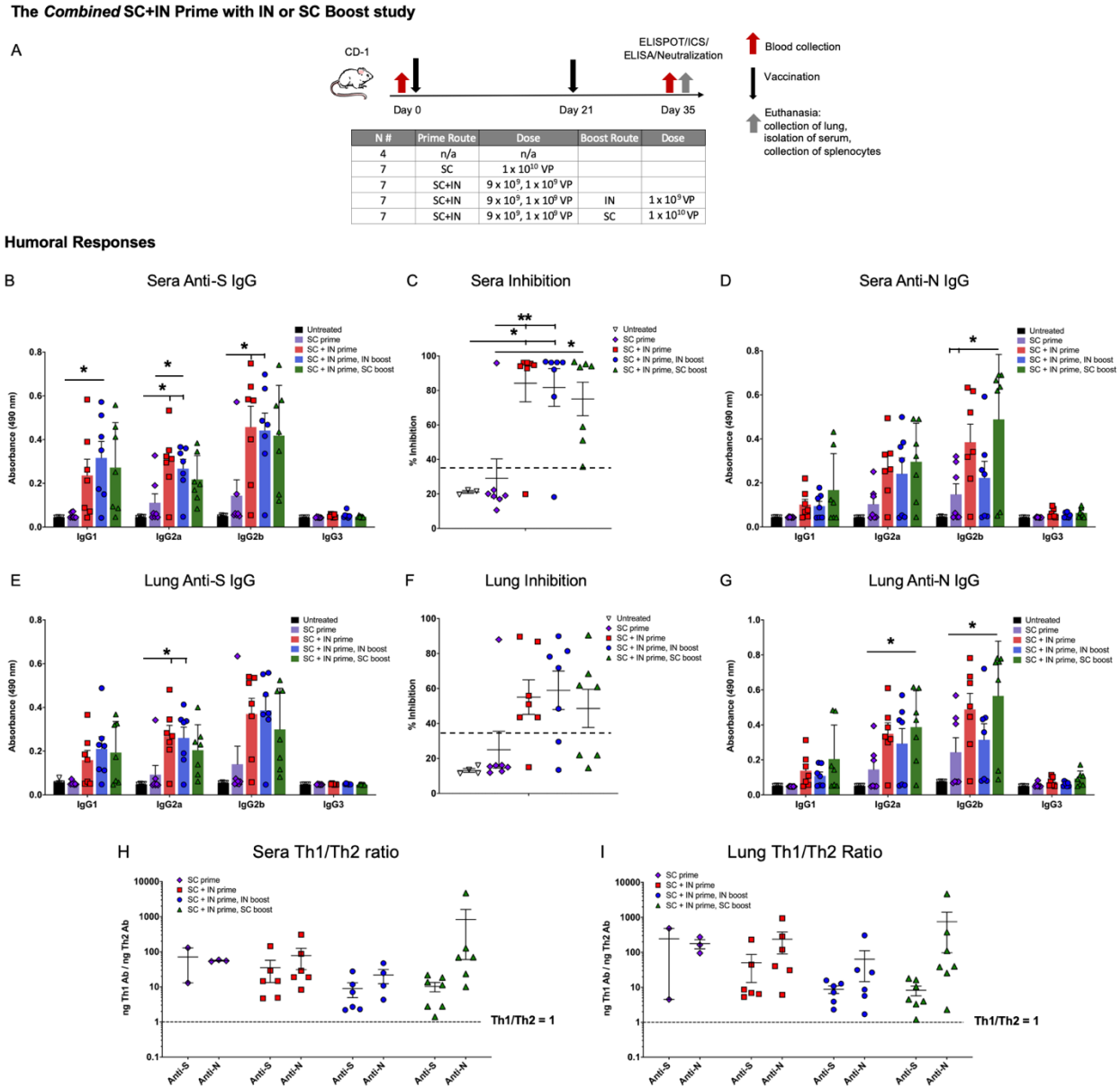

Fig. 5 *Subcutaneous (SC) plus intranasal (IN) prime without boost elicits Th1 dominant neutralizing anti-S and anti-N antibodies.* (A) The study design is shown with groups for SC prime only, SC + IN prime only, and SC + IN prime with either an SC or IN boost, all n = 7. There was an untreated control group (n = 4). Prime dosing was on Day 0, boosts on Day 21, and euthanasia on Day 35. Shown are (B) serum anti-spike (S) antibodies by subtype (dilution 1:30); (C) % inhibition in the surrogate neutralization assay with sera (>35% is correlated with neutralization of virus); and (D) serum anti-nucleocapsid (N) antibodies (dilution 1:270). The same readouts (E) anti-S antibodies; (F) neutralization; and (G) anti-N antibodies are shown for lung homogenate (dilution 1:30 for anti-S and -N). The Th1/Th2 ratios for anti-S and anti-N antibodies are shown for (H) sera and (I) lung. Statistical analyses performed using One-way ANOVA with Tukey's post-hoc analysis comparing treatment groups within each antibody subtype or groups in the neutralization assay where *$p < 0.05$ and ** $p \leq 0.01$.

309 **SC plus IN prime alone without a boost elicits CD4+ T cell responses to N and CD8+ T-cell**
310 **responses to S**

311 Similar to the findings in the first study, ICS shows the N peptide pool stimulated cytokine
312 production by CD4+ T lymphocytes from all vaccinated mice (Fig. 6A-C), but CD8+ T cells from
313 vaccinated mice responded to S peptide pool 1 which contains the S RBD (Fig. 6D-F). The
314 differences between vaccinated groups were not significant due to variability amongst mice, with
315 SC/IN > no boost vaccinated mice having T-cell responses that were similar to those seen with
316 mice that did receive boosts.

317 In ELISpot, the highest IFN-γ secretion in response to peptide pools differed by both peptide
318 pool and vaccination regimen. As compared to the negative control (SIV nef), T cell IFN-γ
319 secretion was significantly greater for the combined SC/IN > SC group in response to the S1
320 peptide pool; greater for the SC/IN > IN group to the S2 peptide pool; and greater for the SC/IN >
321 no boost group to the N peptide pool (Fig. 6G).

322 IL-4 secretion was again very low (Fig. 6H), therefore the IFN-γ/IL-4 ratio was above 1 for
323 all vaccinated mice with only one exception, reflecting Th1 dominance of T-cell responses (Fig.
324 6I).

325

326

327

328

329

330

331

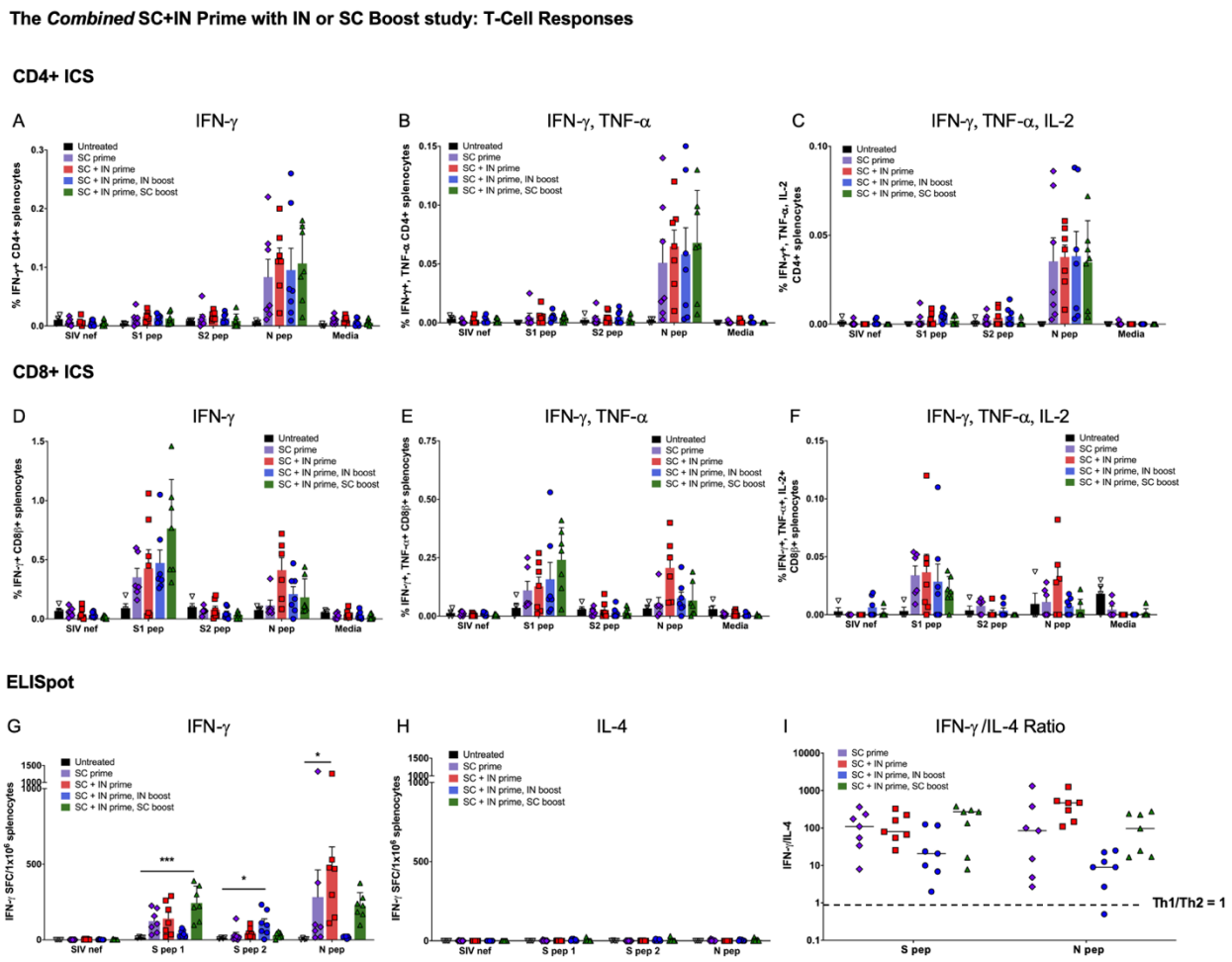

Fig. 6 *CD4+ T-cells respond to nucleocapsid (N) and CD8+ T cells to the spike in the combined SC plus IN prime study with SC or IN boost*. Interferon-γ (IFN-γ); IFN-γ and tumor necrosis factor α (TNF-α); and (C) IFN-γ, TNF-α, and interleukin-2 (IL-2) production by CD4+ (A-C) and CD8+ (D-F) T-cells, respectively, in response to spike 1 (S1, containing the receptor binding domain), S2, and N peptide pools as detected by intracellular cytokine staining (ICS). Some outliers by the Grubb's test were removed. ELISpot for (G) IFN-γ and (H) interleukin-4 (IL-4) secretion in response to the peptide pools. SIV nef and media are negative controls. (I) The IFN-γ/IL-4 ratio showing T helper cell 1 dominance. Statistical analyses performed using One-way ANOVA with Dunnett's post-hoc comparison of each treatment group to untreated for each peptide pool where $*p < 0.05$, $**p \leq 0.01$, and $***p \leq 0.001$.

DISCUSSION

Our hAd5 S-Fusion + N-ETSD vaccine was designed to overcome the risks of an S-only vaccine and elicit both T-cell immunity and neutralizing antibodies, leveraging the vital role T cells play in generating long-lasting antibody responses and in directly killing infected cells. The

348 CD4+ and CD8+ T cells responses induced by this vaccine are multifunctional, and induction of
349 such multifunctional T cells by vaccines is correlated with better protection against infection.[43]
350 We posit that enhanced CD4+ T-cell responses and Th1 predominance resulting from expression
351 of an S antigen optimized for surface display and an N antigen optimized for endosomal/lysosomal
352 subcellular compartment localization and thus MHC I and II presentation, led to increased
353 dendritic cell presentation, cross-presentation, B cell activation, and ultimately high neutralization
354 capability. Furthermore, the potent neutralization capability at high dilution seen for sera from
355 hAd5 S-Fusion + N-ETSD vaccinated mice, combined with Th1 dominance of antibodies
356 generated in response to both S and N antigens, supports the objective of this vaccine design.

357 It is well established that the contemporaneous MHC I and MHC II presentation of an antigen
358 by the antigen presenting cell activates CD4+ and CD8+ T cells simultaneously and is optimal for
359 the generation of memory B and T cells. A key finding of our construct is that N-ETSD, which we
360 show is directed to the endosomal/lysosomal compartment, elicits a CD4+ response, a necessity
361 for induction of memory T cells and helper cells for B cell antibody production. Others have also
362 reported on the importance of lysosomal localization for eliciting the strongest T-cell IFN-γ and
363 CTL responses, compared to natural N.[44,45]

364 The T-cell responses to the S and N antigens expressed by hAd5 S-Fusion + N-ETSD were
365 polycytokine, including IFN-γ, TNF-α, and IL-2 consistent with successful antimicrobial
366 immunity in bacterial and viral infections.[46-50] Post-vaccination polycytokine T-cell responses
367 have been shown to correlate with vaccine efficacy, including those with a viral vector.[43] Highly
368 relevant here, polycytokine T-cell responses to SARS-CoV-2 N protein are consistent with
369 recovered COVID-19 patients,[20] suggesting that the bivalent hAd5 S-Fusion + N-ETSD vaccine
370 will provide vaccine subjects with greater protection against SARS-CoV-2.

371 The key finding here that prime-only vaccination delivered by combination SC and IN dosing
372 results in broad humoral and T-cell responses, with the potential for enhanced mucosal immunity,
373 supports the ongoing clinical testing of the hAd5 S-Fusion + N-ETSD. The vaccine has currently
374 completed Phase 1 testing as an SC prime and SC boost, and oral boost formulations that have
375 shown efficacy in the ability to elicit both humoral and T-cell responses that conferred complete
376 protection against high-titer SARS-CoV-2 challenge in our pre-clinical studies in non-human
377 primates, [1] will soon also be tested in the clinic. To our knowledge, our vaccine is currently the
378 only one available in SC, thermally-stable oral,[51] and IN formulations that offer the expanded
379 possibilities for efficient, feasible delivery across the globe, particularly in developing nations.
380

381 **ACKNOWLEDGEMENTS**

382 We thank Phil Yang of ImmunityBio for his ongoing coordination of project reports for this study.

383

384 **REFERENCES**

385 1 Gabitzsch, E. *et al.* Complete Protection of Nasal and Lung Airways Against SARS-CoV-2
386 Challenge by Antibody Plus Th1 Dominant N- and S-Specific T-Cell Responses to
387 Subcutaneous Prime and Thermally-Stable Oral Boost Bivalent hAd5 Vaccination in an
388 NHP Study. *bioRxiv*, 2020.2012.2008.416297, doi:10.1101/2020.12.08.416297 (2021).
389 2 Sieling, P. *et al.* Th1 Dominant Nucleocapsid and Spike Antigen-Specific CD4+ and CD8+
390 Memory T Cell Recall Induced by hAd5 S-Fusion + N-ETSD Infection of Autologous
391 Dendritic Cells from Patients Previously Infected with SARS-CoV-2. *medRxiv*,
392 2020.2011.2004.20225417, doi:10.1101/2020.11.04.20225417 (2020).
393 3 Amalfitano, A., Begy, C. R. & Chamberlain, J. S. Improved adenovirus packaging cell lines
394 to support the growth of replication-defective gene-delivery vectors. *Proceedings of the*
395 *National Academy of Sciences of the United States of America* **93**, 3352-3356,
396 doi:10.1073/pnas.93.8.3352 (1996).
397 4 Amalfitano, A. *et al.* Production and Characterization of Improved Adenovirus Vectors
398 with the E1, E2b, and E3 Genes Deleted. *Journal of virology* **72**, 926,
399 doi:10.1128/JVI.72.2.926-933.1998 (1998).
400 5 Gatti-Mays, M. E. *et al.* A Phase I Trial Using a Multitargeted Recombinant Adenovirus 5
401 (CEA/MUC1/Brachyury)-Based Immunotherapy Vaccine Regimen in Patients with
402 Advanced Cancer. *Oncologist* **25**, 479, doi:10.1634/theoncologist.2019-0608 (2019).

403 6 Gabitzsch, E. S. *et al.* Anti-tumor immunotherapy despite immunity to adenovirus using
404 a novel adenoviral vector Ad5 [E1-, E2b-]-CEA. *Cancer Immunology, Immunotherapy* **59**,
405 1131-1135, doi:10.1007/s00262-010-0847-8 (2010).
406 7 Gabitzsch, E. S. & Jones, F. R. New recombinant SAd5 vector overcomes Ad5 immunity
407 allowing for multiple safe, homologous, immunizations. *J Clin Cell Immunol* **S4**, 001,
408 doi:doi:10.4172/2155-9899 (2011).
409 8 Gabitzsch, E. S. *et al.* Anti-tumor immunotherapy despite immunity to adenovirus using
410 a novel adenoviral vector Ad5 [E1-, E2b-]-CEA. *Cancer immunology, immunotherapy : CII*
411 **59**, 1131-1135, doi:10.1007/s00262-010-0847-8 (2010).
412 9 Wrapp, D. *et al.* Cryo-EM structure of the 2019-nCoV spike in the prefusion
413 conformation. *Science* **367**, 1260-1263, doi:10.1126/science.abb2507 (2020).
414 10 Lu, R. *et al.* Genomic characterisation and epidemiology of 2019 novel coronavirus:
415 implications for virus origins and receptor binding. *Lancet (London, England)* **395**, 565-
416 574, doi:10.1016/S0140-6736(20)30251-8 (2020).
417 11 Walls, A. C. *et al.* Structure, Function, and Antigenicity of the SARS-CoV-2 Spike
418 Glycoprotein. *Cell* **181**, 281-292.e286, doi:10.1016/j.cell.2020.02.058 (2020).
419 12 Hamming, I. *et al.* Tissue distribution of ACE2 protein, the functional receptor for SARS
420 coronavirus. A first step in understanding SARS pathogenesis. *J Pathol* **203**, 631-637,
421 doi:10.1002/path.1570 (2004).
422 13 Tai, W. *et al.* Characterization of the receptor-binding domain (RBD) of 2019 novel
423 coronavirus: implication for development of RBD protein as a viral attachment inhibitor
424 and vaccine. *Cell Mol Immunol*, doi:10.1038/s41423-020-0400-4 (2020).
425 14 Suthar, M. S. *et al.* Rapid generation of neutralizing antibody responses in COVID-19
426 patients. *Cell Reports Medicine*, doi:10.1016/j.xcrm.2020.100040.
427 15 Grifoni, A. *et al.* Targets of T Cell Responses to SARS-CoV-2 Coronavirus in Humans with
428 COVID-19 Disease and Unexposed Individuals. *Cell* **181**, 1489,
429 doi:10.1016/j.cell.2020.05.015 (2020).
430 16 Tegally, H. *et al.* Sixteen novel lineages of SARS-CoV-2 in South Africa. *Nature Medicine*,
431 doi:10.1038/s41591-021-01255-3 (2021).
432 17 Leung, K., Shum, M. H., Leung, G. M., Lam, T. T. & Wu, J. T. Early transmissibility
433 assessment of the N501Y mutant strains of SARS-CoV-2 in the United Kingdom, October
434 to November 2020. *Euro Surveill* **26**, doi:10.2807/1560-7917.Es.2020.26.1.2002106
435 (2021).
436 18 Davies, N. G. *et al.* Estimated transmissibility and severity of novel SARS-CoV-2 Variant
437 of Concern 202012/01 in England. *medRxiv*, 2020.2012.2024.20248822,
438 doi:10.1101/2020.12.24.20248822 (2020).
439 19 Zhang, W. *et al.* Emergence of a Novel SARS-CoV-2 Variant in Southern California. *JAMA*,
440 doi:10.1001/jama.2021.1612 (2021).
441 20 Peng, H. *et al.* Long-lived memory T lymphocyte responses against SARS coronavirus
442 nucleocapsid protein in SARS-recovered patients. *Virology* **351**, 466-475,
443 doi:https://doi.org/10.1016/j.virol.2006.03.036 (2006).
444 21 Shang, B. *et al.* Characterization and application of monoclonal antibodies against N
445 protein of SARS-coronavirus. *Biochemical and Biophysical Research Communications*
446 **336**, 110-117, doi:https://doi.org/10.1016/j.bbrc.2005.08.032 (2005).

447 22 Azizi, A. *et al.* A combined nucleocapsid vaccine induces vigorous SARS-CD8+ T-cell
448 immune responses. *Genet Vaccines Ther* **3**, 7, doi:10.1186/1479-0556-3-7 (2005).
449 23 Zeng, W. *et al.* Biochemical characterization of SARS-CoV-2 nucleocapsid protein.
450 *Biochemical and biophysical research communications*, S0006-0291X(0020)30876-
451 30877, doi:10.1016/j.bbrc.2020.04.136 (2020).
452 24 Narayanan, K., Chen, C.-J., Maeda, J. & Makino, S. Nucleocapsid-independent specific
453 viral RNA packaging via viral envelope protein and viral RNA signal. *Journal of virology*
454 **77**, 2922-2927, doi:10.1128/jvi.77.5.2922-2927.2003 (2003).
455 25 McBride, R., van Zyl, M. & Fielding, B. C. The coronavirus nucleocapsid is a
456 multifunctional protein. *Viruses* **6**, 2991-3018, doi:10.3390/v6082991 (2014).
457 26 Nisreen, M. A. O. *et al.* Severe Acute Respiratory Syndrome Coronavirus 2–Specific
458 Antibody Responses in Coronavirus Disease 2019 Patients. *Emerging Infectious Disease*
459 *journal* **26**, 1478-1488, doi:10.3201/eid2607.200841 (2020).
460 27 Long, Q.-X. *et al.* Antibody responses to SARS-CoV-2 in patients with COVID-19. *Nature*
461 *Medicine*, doi:10.1038/s41591-020-0897-1 (2020).
462 28 Altmann, D. M. & Boyton, R. J. SARS-CoV-2 T cell immunity: Specificity, function,
463 durability, and role in protection. *Sci Immunol* **5**, doi: 10.1126/sciimmunol.abd6160,
464 doi:10.1126/sciimmunol.abd6160 (2020).
465 29 Ni, L. *et al.* Detection of SARS-CoV-2-Specific Humoral and Cellular Immunity in COVID-
466 19 Convalescent Individuals. *Immunity*, doi:10.1016/j.immuni.2020.04.023 (2020).
467 30 Weiskopf, D. *et al.* Phenotype and kinetics of SARS-CoV-2–specific T cells in COVID-19
468 patients with acute respiratory distress syndrome. *Science Immunology* **5**, eabd2071,
469 doi:10.1126/sciimmunol.abd2071 (2020).
470 31 Ng, O. W. *et al.* Memory T cell responses targeting the SARS coronavirus persist up to 11
471 years post-infection. *Vaccine* **34**, 2008-2014, doi:10.1016/j.vaccine.2016.02.063 (2016).
472 32 Tang, F. *et al.* Lack of peripheral memory B cell responses in recovered patients with
473 severe acute respiratory syndrome: a six-year follow-up study. *Journal of immunology*
474 *(Baltimore, Md. : 1950)* **186**, 7264-7268, doi:10.4049/jimmunol.0903490 (2011).
475 33 Le Bert, N. *et al.* SARS-CoV-2-specific T cell immunity in cases of COVID-19 and SARS, and
476 uninfected controls. *Nature* **584**, 457, doi:10.1038/s41586-020-2550-z (2020).
477 34 Sekine, T. *et al.* Robust T cell immunity in convalescent individuals with asymptomatic or
478 mild COVID-19. *Cell* **183**, 158, doi:10.1101/2020.06.29.174888 (2020).
479 35 Vabret, N. Antibody responses to SARS-CoV-2 short-lived. *Nature Reviews Immunology*,
480 doi:10.1038/s41577-020-0405-3 (2020).
481 36 Polack, F. P. *et al.* Safety and Efficacy of the BNT162b2 mRNA Covid-19 Vaccine. *N Engl J*
482 *Med* **383**, 2603-2615, doi:10.1056/NEJMoa2034577 (2020).
483 37 Baden, L. R. *et al.* Efficacy and Safety of the mRNA-1273 SARS-CoV-2 Vaccine. *N Engl J*
484 *Med* **384**, 403-416, doi:10.1056/NEJMoa2035389 (2021).
485 38 Magrone, T., Magrone, M. & Jirillo, E. Focus on Receptors for Coronaviruses with Special
486 Reference to Angiotensin- Converting Enzyme 2 as a Potential Drug Target - A
487 Perspective. *Endocr Metab Immune Disord Drug Targets* **20**, 807-811,
488 doi:10.2174/1871530320666200427112902 (2020).

489 39 Fehr, A. R. & Perlman, S. Coronaviruses: an overview of their replication and
490 pathogenesis. *Methods in molecular biology (Clifton, N.J.)* **1282**, 1-23, doi:10.1007/978-
491 1-4939-2438-7_1 (2015).
492 40 Bourouiba, L. Turbulent Gas Clouds and Respiratory Pathogen Emissions: Potential
493 Implications for Reducing Transmission of COVID-19. *Jama* **323**, 1837-1838,
494 doi:10.1001/jama.2020.4756 (2020).
495 41 Sterlin, D. *et al.* IgA dominates the early neutralizing antibody response to SARS-CoV-2.
496 *Sci Transl Med* **13**, doi:10.1126/scitranslmed.abd2223 (2021).
497 42 Tan, C. W. *et al.* A SARS-CoV-2 surrogate virus neutralization test based on antibody-
498 mediated blockage of ACE2-spike protein-protein interaction. *Nat Biotechnol* **38**, 1073-
499 1078, doi:10.1038/s41587-020-0631-z (2020).
500 43 Darrah, P. A. *et al.* Multifunctional TH1 cells define a correlate of vaccine-mediated
501 protection against Leishmania major. *Nat Med* **13**, 843-850, doi:10.1038/nm1592
502 (2007).
503 44 Gupta, V. *et al.* SARS coronavirus nucleocapsid immunodominant T-cell epitope cluster
504 is common to both exogenous recombinant and endogenous DNA-encoded
505 immunogens. *Virology* **347**, 127-139, doi:10.1016/j.virol.2005.11.042 (2006).
506 45 Yang, K. *et al.* Immune responses to T-cell epitopes of SARS CoV-N protein are enhanced
507 by N immunization with a chimera of lysosome-associated membrane protein. *Gene*
508 *Ther* **16**, 1353-1362, doi:10.1038/gt.2009.92 (2009).
509 46 Lichterfeld, M. *et al.* HIV-1-specific cytotoxicity is preferentially mediated by a subset of
510 CD8(+) T cells producing both interferon-gamma and tumor necrosis factor-alpha. *Blood*
511 **104**, 487-494, doi:10.1182/blood-2003-12-4341 (2004).
512 47 Betts, M. R. *et al.* HIV nonprogressors preferentially maintain highly functional HIV-
513 specific CD8+ T cells. *Blood* **107**, 4781-4789, doi:10.1182/blood-2005-12-4818 (2006).
514 48 Cox, M. A. & Zajac, A. J. Shaping successful and unsuccessful CD8 T cell responses
515 following infection. *J Biomed Biotechnol* **2010**, 159152-159152,
516 doi:10.1155/2010/159152 (2010).
517 49 Rosendahl Huber, S., van Beek, J., de Jonge, J., Luytjes, W. & van Baarle, D. T cell
518 responses to viral infections - opportunities for Peptide vaccination. *Front Immunol* **5**,
519 171-171, doi:10.3389/fimmu.2014.00171 (2014).
520 50 Seder, R. A., Darrah, P. A. & Roederer, M. T-cell quality in memory and protection:
521 implications for vaccine design. *Nat Rev Immunol* **8**, 247-258, doi:10.1038/nri2274
522 (2008).
523 51 Stewart, M., Ward, S. J. & Drew, J. Use of adenovirus as a model system to illustrate a
524 simple method using standard equipment and inexpensive excipients to remove live
525 virus dependence on the cold-chain. *Vaccine* **32**, 2931-2938,
526 doi:10.1016/j.vaccine.2014.02.033 (2014).
527 52 Zhu, F.-C. *et al.* Safety, tolerability, and immunogenicity of a recombinant adenovirus
528 type-5 vectored COVID-19 vaccine: a dose-escalation, open-label, non-randomised, first-
529 in-human trial. *The Lancet*, doi:10.1016/S0140-6736(20)31208-3.
530 53 van Doremalen, N. *et al.* ChAdOx1 nCoV-19 vaccination prevents SARS-CoV-2
531 pneumonia in rhesus macaques. *bioRxiv*, 2020.2005.2013.093195,
532 doi:10.1101/2020.05.13.093195 (2020).

533 54 Amalfitano, A. & Chamberlain, J. S. Isolation and characterization of packaging cell lines
534 that coexpress the adenovirus E1, DNA polymerase, and preterminal proteins:
535 implications for gene therapy. *Gene Ther* **4**, 258-263, doi:10.1038/sj.gt.3300378 (1997).
536 55 Seregin, S. S. & Amalfitano, A. Overcoming pre-existing adenovirus immunity by genetic
537 engineering of adenovirus-based vectors. *Expert Opin Biol Ther* **9**, 1521-1531,
538 doi:10.1517/14712590903307388 (2009).
539 56 Srinivasan, S. *et al.* Structural Genomics of SARS-CoV-2 Indicates Evolutionary Conserved
540 Functional Regions of Viral Proteins. *Viruses* **12**, 360, doi:10.3390/v12040360 (2020).
541 57 Schaack, J. *et al.* Promoter strength in adenovirus transducing vectors: down-regulation
542 of the adenovirus E1A promoter in 293 cells facilitates vector construction. *Virology* **291**,
543 101-109, doi:10.1006/viro.2001.1211 (2001).
544 58 Tan, C. W. *et al.* A SARS-CoV-2 surrogate virus neutralization test based on antibody-
545 mediated blockage of ACE2-spike protein-protein interaction. *Nat Biotechnol*,
546 doi:10.1038/s41587-020-0631-z (2020).
547
548
549
550
551
552
553
554
555
556
557
558
559
560
561
562
563

564 **SUPPLEMENTARY INFORMATION**
565
566 **METHODS**
567
568 *The hAd5 [E1-, E2b-, E3-] platform and constructs*
569
570 For studies here, the next generation hAd5 [E1-, E2b-, E3-] vector was used (Fig. S1A) to
571 create viral vaccine candidate constructs. This hAd5 [E1-, E2b-, E3-] vector is primarily
572 distinguished from other first-generation [E1-, E3-] recombinant Ad5 platforms [52,53] by having
573 additional deletions in the early gene 2b (E2b) region that remove the expression of the viral DNA
574 polymerase (pol) and in pre terminal protein (pTP) genes, and its propagation in the E.C7 human
575 cell line.[3,4,54,55]
576 The hAd5 S-Fusion + N-ETSD vaccine we utilized the hAd5 [E1-, E2b-, E3-] comprises a
577 wildtype spike (S) sequence [accession number YP009724390] modified with a proprietary linker
578 peptide sequence as well as a wildtype nucleocapsid (N) sequence [accession number
579 YP009724397] with a an Enhanced T-cell Stimulation Domain (ETSD) signal sequence to direct
580 translated N to the endosomal/lysosomal pathway. [2] The SARS-CoV-2 S protein is found on the
581 viral surface [11] and the N protein is found in the interior of the virus [23,56] (Fig. S1B).
582 The powerful cytomegalovirus (CMV) promoter [57] drives expression in the hAd5 construct
583 (Fig. S1C).
584

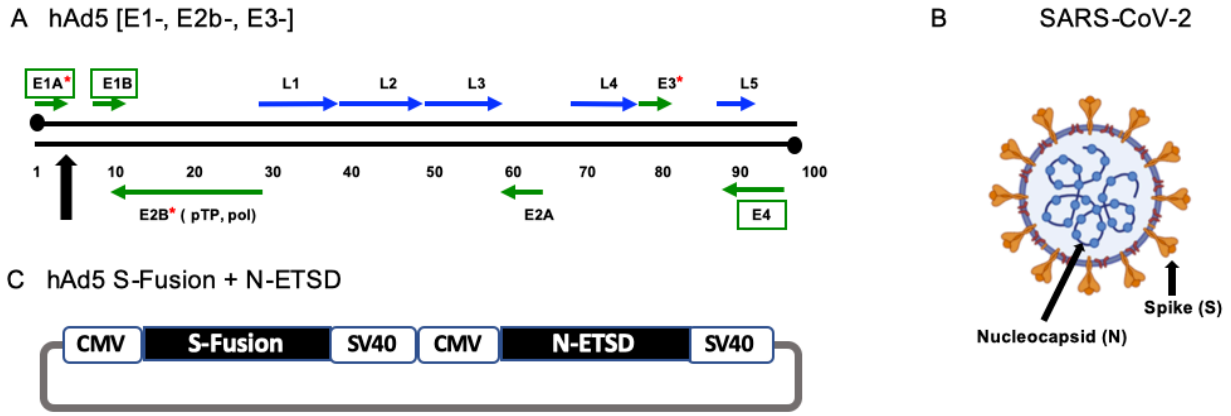

585
586 **Fig. S1** *The SARS-CoV-2 virus, the hAd5 [E1-, E2b-, E3-] vector and the dual antigen hAd5 S-*
587 *Fusion + N-ETSD vaccine.* (A) The second-generation human adenovirus serotype 5 (hAd5)
588 vector used has the E1, E2b, and E3 regions deleted. Sequences for the vaccine antigen cargo are
589 inserted at the black arrow. (B) The spike (S) glycoprotein is displayed as a trimer on the surface
590 of SARS-CoV-2 and the nucleocapsid (N) protein is found in the virus interior, associated with
591 the viral RNA. (C) The vaccine antigens are under control of the cytomegalovirus (CMV) promoter
592 and sequences end with SV40 poly-A.
593
594 *Transfection of HEK 293T cells with hAd5 constructs and flow cytometric analysis of RBD*
595 *surface expression*
596
597 To determine surface expression of the RBD epitope by vaccine candidate constructs, we
598 transfected HEK 293T cells with hAd5 construct DNA and quantified surface RBD by flow
599 cytometric detection using anti-RBD antibodies. The constructs tested were: S-WT, S-WT + N-

600 ETSD, S-Fusion, S-Fusion + N-ETSD, and N-ETSD. HEK 293T cells (2.5 x 10^5 cells/well in 24
601 well plates) were grown in DMEM (Gibco Cat# 11995-065) with 10% FBS and 1X PSA (100
602 units/mL penicillin, 100 μg/mL streptomycin, 0.25 ug/mL Amphotericin B) at 37°C. Cells were
603 transfected with 0.5 μg of hAd5 plasmid DNA using a JetPrime transfection reagent (Polyplus
604 Catalog # 89129-924) according to the manufacturer's instructions. Cells were harvested 1, 2, 3,
605 and 7 days post transfection by gently pipetting cells into medium and labeled with an anti-RBD
606 monoclonal antibody (clone D003 Sino Biological Catalog # 40150-D003) and F(ab')2-Goat anti-
607 Human IgG-Fc secondary antibody conjugated with R-phycoerythrin (ThermoFisher Catalog #
608 H10104). Labeled cells were acquired using a Thermo-Fisher Attune NxT flow cytometer and
609 analyzed using Flowjo Software.
610
611 *ACE2-IgG1Fc binding to hAd5 transfected HEK 293T cells*
612
613 HEK 293T cells were cultured at 37°C under conditions described above for transfection with
614 hAd5 S-WT, S-Fusion, and S-Fusion + N-ETSD and were incubated for 2 days and harvested for
615 ACE2-Fc binding analysis. Recombinant ACE2-IgG1Fc protein was produced using Maxcyte
616 transfection in CHO-S cells that were cultured for 14 days. ACE2-IgG1Fc was then purified using
617 a MabSelect SuRe affinity column on AKTA Explorer. Purified ACE2-IgG1Fc was dialyzed into
618 10 mM HEPES, pH7.4, 150 mM NaCl and concentrated to 2.6 mg/mL. For binding studies, the
619 ACE2-IgG1Fc was used at a concentration of 1 μg/mL for binding. Cells were incubated with
620 ACE2-Fc for 20 minutes and, after a washing step, were then labeled with a PE conjugated F(ab')2-
621 goat anti-human IgG Fc secondary antibody at a 1:100 dilution, incubated for 20 minutes, washed
622 and acquired on flow cytometer. Histograms are based on normalized mode (NM) of cell count –
623 count of cells positive for signal in PE channel.
624
625 *Murine immunization and blood/tissue collection*
626
627 CD-1 female mice (Charles River Laboratories) 6-8 weeks of age were used for
628 immunological studies performed at the vivarium facilities of Omeros Inc. (Seattle, WA). Mice
629 were administered subcutaneous (SC) injections at the indicated doses in 50 μL ARM buffer (20
630 mM Tris pH 8.0, 25 mM NaCl, with 2.5% glycerol) or intranasal (IN) injections at the indicated
631 doses in 10 μL ARM buffer (5 μL per nostril) while under isoflurane anesthesia. On the final day
632 of each study, blood was collected via the submandibular vein from isoflurane-anesthetized mice
633 for isolation of sera using a microtainer tube and then mice were euthanized for collection of spleen
634 and lungs.
635 Spleens were removed from each mouse and placed in 5 mL of sterile media
636 (RPMI/HEPES/Pen/Strep/10% FBS). Splenocytes were isolated within 2 hours of collection and
637 used fresh or frozen for later analysis.
638 Lungs were removed from each mouse, dissected in half and then immediately snap frozen
639 on dry ice. Lung homogenates were generated by thawing one frozen lung half and homogenizing
640 in 150 μL sterile PBS using a Fisher Scientific pestle drill. Homogenates were centrifuged at
641 13,000 rpm for 3 minutes and supernatants were utilized in ELISA and cPass surrogate
642 neutralization assays.
643
644 *Intracellular cytokine stimulation (ICS)*
645

646 ICS assays were performed using 10^6 live splenocytes per well in 96-well U-bottom plates.
647 Splenocytes in RPMI media supplemented with 10% FBS were stimulated by the addition of pools
648 of overlapping peptide for S or N antigens at 2 μg/mL/peptide for 6 h at 37°C in 5% CO_2, with
649 protein transport inhibitor, GolgiStop (BD) added two hours after initiation of incubation. The S
650 peptide pool (JPT: Cat #PM-WCPV-S-1) is a total of 315 spike peptides split into two pools
651 comprised of 158 and 157 peptides each. The N peptide pool (JPT; Cat # PM-WCPV-NCAP-1)
652 was also used to stimulate cells. A SIV-Nef peptide pool (BEI Resources) was used as an off-target
653 negative control. Stimulated splenocytes were then stained for a fixable cell viability stain
654 followed by the lymphocyte surface markers CD8β and CD4, fixed with CytoFix (BD),
655 permeabilized, and stained for intracellular accumulation of IFN-γ, TNF-α and IL-2 (in studies 2
656 and 3). Fluorescent-conjugated antibodies against mouse CD8β antibody (clone H35-17.2,
657 ThermoFisher), CD4 (clone RM4-5, BD), IFN-γ (clone XMG1.2, BD), TNF-α (clone MP6-XT22,
658 BD) and IL-2 (clone JES6-5H4; BD), and staining was performed in the presence of unlabeled
659 anti-CD16/CD32 antibody (clone 2.4G2; BD). Flow cytometry was performed using a Beckman-
660 Coulter Cytoflex S flow cytometer and analyzed using Flowjo Software.
661
662 *ELISpot assay*
663
664 ELISpot assays were used to detect cytokines secreted by splenocytes from inoculated mice.
665 Fresh splenocytes were used on the same day, as were cryopreserved splenocytes containing
666 lymphocytes. The cells (2-4 x 10^5 cells per well of a 96-well plate) were added to the ELISpot
667 plate containing an immobilized primary antibodies to either IFN-γ or IL-4 (BD), and were
668 exposed to various stimuli (e.g. control peptides, target peptide pools/proteins) comprising 2
669 μg/mL peptide pools or 10 μg/mL protein for 36-40 hours. After aspiration and washing to remove
670 cells and media, extracellular cytokine was detected by a secondary antibody to cytokine
671 conjugated to biotin (BD). A streptavidin/horseradish peroxidase conjugate was used detect the
672 biotin-conjugated secondary antibody. The number of spots per well, or per 2-4 x 10^5 cells, was
673 counted using an ELISpot plate reader. A Th1/Th2 ratio was calculated by dividing the IFN-γ spot
674 forming cells (SFC) per million splenocytes with the IL-4 SFC per million splenocytes for each
675 animal.
676
677 *ELISA for detection of antibodies*
678
679 For IgG antibody detection in sera and lung homogenate from inoculated mice, ELISAs
680 specific for spike and nucleocapsid antibodies, as well as for IgG subtype (IgG1, IgG2a, IgG2b,
681 and IgG3) antibodies were used. In addition, for IgA antibody detection in lung homogenate from
682 inoculated mice, ELISAs specific for spike and nucleocapsid antibodies, as well as for IgA was
683 used. A microtiter plate was coated overnight with 100 ng of either purified recombinant SARS-
684 CoV-2 S-FTD (full-length S with fibritin trimerization domain, constructed and purified in-house
685 by ImmunityBio), SARS-CoV-2 S RBD (Sino Biological, Beijing, China; Cat # 401591-V08B1-
686 100) or purified recombinant SARS-CoV-2 nucleocapsid (N) protein (Sino Biological, Beijing,
687 China; Cat # 40588-V08B) in 100 μL of coating buffer (0.05 M Carbonate Buffer, pH 9.6). The
688 wells were washed three times with 250 μL PBS containing 1% Tween 20 (PBST) to remove
689 unbound protein and the plate was blocked for 60 minutes at room temperature with 250 μL PBST.
690 After blocking, the wells were washed with PBST, 100 μL of either diluted serum or diluted lung
691 homogenate samples were added to wells, and samples incubated for 60 minutes at room
692 temperature. After incubation, the wells were washed with PBST and 100 μL of a 1/5000 dilution

693 of anti-mouse IgG HRP (GE Health Care; Cat # NA9310V), or anti-mouse IgG_1 HRP (Sigma; Cat
694 # SAB3701171), or anti-mouse IgG_{2a} HRP (Sigma; Cat # SAB3701178), or anti-mouse IgG_{2b} HRP
695 (Sigma; catalog# SAB3701185), anti-mouse IgG_3 HRP conjugated antibody (Sigma; Cat #
696 SAB3701192), or anti-mouse IgA HRP conjugated antibody (Sigma; Cat # A4789) was added to
697 wells. For positive controls, a 100 µL of a 1/5000 dilution of rabbit anti-N IgG Ab or 100 µL of a
698 1/25 dilution of mouse anti-S serum (from mice immunized with purified S antigen in adjuvant)
699 were added to appropriate wells. After incubation at room temperature for 1 hour, the wells were
700 washed with PBS-T and incubated with 200 µL o-phenylenediamine-dihydrochloride (OPD
701 substrate (Thermo Scientific Cat # A34006) until appropriate color development. The color
702 reaction was stopped with addition of 50 µL 10% phosphoric acid solution (Fisher Cat # A260-
703 500) in water and the absorbance at 490 nm was determined using a microplate reader (SoftMax®
704 Pro, Molecular Devices).
705
706 *Calculation of relative ng amounts of antibodies and the Th1/Th2 ratio*
707
708 A standard curve of IgG was generated and absorbance values were converted into mass
709 equivalents for both anti-S and anti-N antibodies. Using these values, we were able to calculate
710 that hAd5 S-Fusion + N-ETSD vaccination generated a geometric mean value for S- and N-
711 specific IgG per milliliter of serum. These values were also used to generate a Th1/Th2 ratio for
712 the humoral responses by dividing the sum total of Th1 skewed antigen-specific IgG isotypes
713 (IgG2a, IgG2b and IgG3) with the total Th2 skewed IgG3, for each mouse. Some responses,
714 particularly for anti-N responses in IgG2a and IgG2b (both Th1 skewed isotypes), were above the
715 limit of quantification with OD values higher than those observed in the standard curve. These
716 data points were reduced to values within the standard curve, and thus will reflect a lower Th1/Th2
717 skewing than would otherwise be reported.
718
719 *cPass™ neutralizing antibody detection*
720
721 The GenScript cPass™ (https://www.genscript.com/cpass-sars-cov-2-neutralization-
722 antibody-detection-Kit.html) for detection of neutralizing antibodies was used according to the
723 manufacturer's instructions.[58] The kit detects circulating neutralizing antibodies against SARS-
724 CoV-2 that block the interaction between the S RBD with the ACE2 cell surface receptor. It is
725 suitable for all antibody isotypes and appropriate for use with in animal models without
726 modification.
727
728 *Vero E6 cell neutralization assay*
729
730 All aspects of the assay utilizing virus were performed in a BSL3 containment facility
731 according to the ISMMS Conventional Biocontainment Facility SOPs for SARS-CoV-2 cell
732 culture studies. Vero e6 kidney epithelial cells from *Cercopithecus aethiops* (ATCC CRL-1586)
733 were plated at 20,000 cells/well in a 96-well format and 24 hours later, cells were incubated with
734 antibodies or heat inactivated sera previously serially diluted in 3-fold steps in DMEM containing
735 2% FBS, 1% NEAAs, and 1% Pen-Strep; the diluted samples were mixed 1:1 with SARS-CoV-2
736 in DMEM containing 2% FBS, 1% NEAAs, and 1% Pen-Strep at 10,000 TCID50/mL for 1 hr. at
737 37°C, 5% CO_2. This incubation did not include cells to allow for neutralizing activity to occur
738 prior to infection. The samples for testing included sera from the four mice that showed anti-S
739 IgG2a and IgG2b antibody responses in Fig. 1B, pooled sera from those four mice, sera from a

740 COVID-19 convalescent patient, and media only. For detection of neutralization, 120 μL of the
741 virus/sample mixture was transferred to the Vero E6 cells and incubated for 48 hours before
742 fixation with 4% PFA. Each well received 60 μL of virus or an infectious dose of 600 TCID50.
743 Control wells including 6 wells on each plate for no virus and virus-only controls were used. The
744 percent neutralization was calculated as 100-((sample of interest-[average of "no virus"])/[average
745 of "virus only"])*100) with a stain for CoV-2 Np imaged on a Celigo Imaging Cytometer
746 (Nexcelom Bioscience).
747
748 **SUPPLEMENTARY RESULTS**
749
750 **Enhanced HEK 293T cell-surface expression of RBD following transfection with Ad5 S-**
751 **Fusion + N-ETSD**
752
753 As shown in Figure S2, anti-RBD-specific antibodies did not detect RBD on the surface of
754 HEK 293T cells transfected with hAd5 S-WT (Fig. 2A) or hAd5 S-WT + N-ETSD (Fig. 2B)
755 constructs, while hAd5 S-Fusion alone was higher (Fig. 2C). Notably, the highest cell-surface
756 expression of RBD was detected after transfection with dual antigen hAd5 S-Fusion + N-ETSD
757 (Fig. 2D). Similar results were seen for recombinant ACE2-Fc binding to S-WT, S-Fusion and S-
758 Fusion + N-ETSD, with ACE2 showing higher binding to S-Fusion than S-WT and the dual
759 antigen construct showing the highest binding (Fig. S2F-H). These findings support our
760 proposition that an hAd5 S-Fusion + N-ETSD construct, containing a high number and variety of
761 antigens provided by both full-length, optimized S with proper folding and N leads to enhanced
762 expression and cell surface display of RBD in a vaccine construct.
763

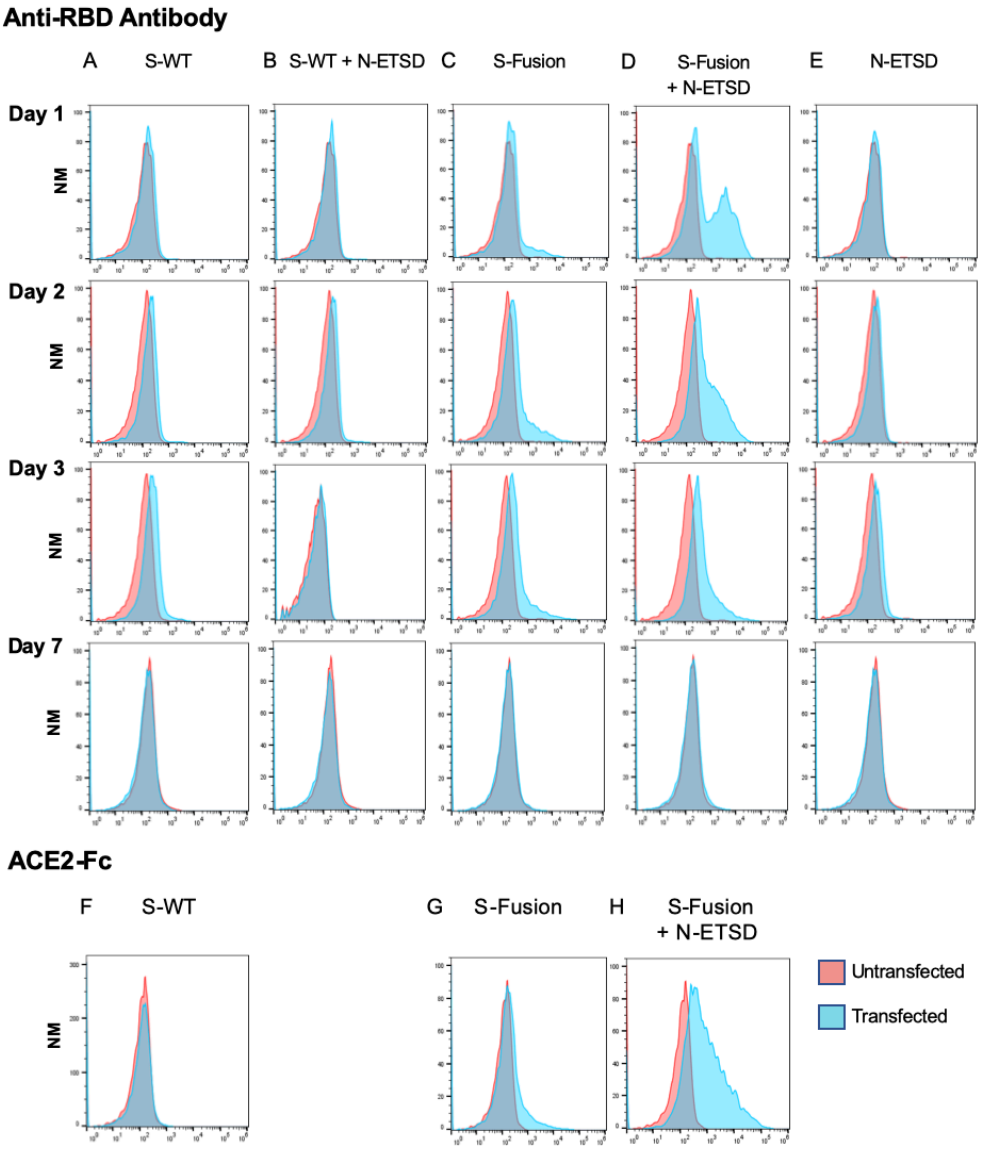

764
765 **Fig. S2** *Transfection of HEK293T cells with hAd5 S-Fusion + ETSD results in enhanced surface*
766 *expression of the spike receptor binding domain (RBD).* Flow cytometric analysis of an anti-RBD
767 antibody with construct-transfected cells reveals no detectable surface expression of RBD in either
768 (A) S-WT or (B) S-WT + N-ETSD transfected cells. Expression was higher in (C) S-Fusion
769 transfected cells as compared to S-WT. Cell surface expression of the RBD was high in (D) S-
770 Fusion + N-ETSD transfected cells, particularly at day 1 and 2. (E) No expression was detected
771 the N-ETSD negative control. Recombinant ACE2-Fc binding to (F) S-WT, (G) and S-Fusion, and
772 (H) S-Fusion + N-ETSD is shown. Y-axis scale is normalized to mode (NM).